
Out-of-Distribution Detection with Class Ratio Estimation

Mingtian Zhang^{14*} Andi Zhang^{24*} Tim Z. Xiao³ Yitong Sun⁴ Steven McDonagh⁴

¹Centre for Artificial Intelligence, University College London

²Department of Computer Science and Technology, University of Cambridge

³University of Tübingen & IMPRS-IS ⁴Huawei Noah's Ark Lab,

m.zhang@cs.ucl.ac.uk az381@cam.ac.uk zhenzhong.xiao@uni-tuebingen.de
{sunityong, steven.mcdonagh}@huawei.com

Abstract

Density-based Out-of-distribution (OOD) detection has recently been shown unreliable for the task of detecting OOD images. Various density ratio based approaches achieve good empirical performance, however methods typically lack a principled probabilistic modelling explanation. In this work, we propose to unify density ratio based methods under a novel framework that builds energy-based models and employs differing base distributions. Under our framework, the density ratio can be viewed as the unnormalized density of an implicit semantic distribution. Further, we propose to directly estimate the density ratio of a data sample through class ratio estimation. We report competitive results on OOD image problems in comparison with recent work that alternatively requires training of deep generative models for the task. Our approach enables a simple and yet effective path towards solving the OOD detection problem.

1 Background

Machine learning methods often assume that training and testing data originate from the same distribution. However, in many real world applications, we usually have little control over the data source. Therefore, detecting Out-of-distribution (OOD) data is critical for safe and reliable machine learning applications. The importance of the problem has led to the design of many methods which aim to tackle OOD detection.

Several works study the OOD detection problem in the scenario where both the in-distribution (ID) data and corresponding labels are presented. For example, [13] presents a practical baseline for OOD detection using a softmax confidence score. A selection of follow-up works then propose various routes to improve the performance of OOD detection *e.g.* using neural network calibration [9, 19], deep ensembles [21], the ODIN score [24], the Mahalanobis distance [23], energy based scores [25] and Gram Matrices [38]. However, different classes of labels require the classifier to encode different features. As a thought experiment, consider being given MNIST digits with binary labels that represent ‘*if the 100th pixel is black or not*’. Features learned by a resulting classifier will clearly not capture any semantic information pertaining to digits. Therefore, approaches of this type strongly rely on the labels’ quality, and we refer to this strategy as ‘label-dependent OOD detection’.

Alternatively, OOD detection can be performed without labels, where we hope the detector can distinguish between the ID and OOD data by using their ‘semantics’ [34, 11]. Compared to label-dependent OOD, this type of OOD detection is more consistent with human intuition and can

*Equal Contribution, the work was done during an internship in Huawei Noah's Ark Lab.

potentially exhibit better generalisation and robustness. One historically popular approach is to formalise the unsupervised OOD task as a density estimation problem [2], which usually includes training a model on the ID data and using the evaluated density as the score for the OOD detection task. However, recent work [30] shows that for popular deep generative models, OOD data may have a higher density (likelihood) value than ID data, which makes OOD detection fail. Investigating further, various papers make proposals: typical sets [31], dataset complexity [40], inductive bias [17], likelihood domination [39, 49] towards explaining this phenomenon, yet the fundamental reasons underlying why deep generative models fail to detect OOD datasets remain not fully understood [17].

Recently, many density ratio methods have been proposed to resolve this challenge [34, 17, 11, 50], where the ratio between density values, which are evaluated by two models respectively, is used as the score function for the OOD detection. Although good empirical results are achieved in practice, such approaches usually lack a principled modelling explanation. Additionally, we observe the proposed methods all require training exactly one or two generative models, which is computationally expensive and potentially redundant if the goal is to estimate the density ratios. Therefore, in this work, we aim to understand the density ratio-based methods from a modelling perspective and show how to estimate the density without training generative models.

Explicitly, our main contributions are as follows:

- We unify the existing density ratio based OOD detection methods as building energy based models on the in-distribution data.
- We propose to use class ratio estimation to evaluate density ratios with a binary classifier. This significantly simplifies the procedure of learning an OOD detector yet retains competitive performance.
- Through the consideration of a classical class ratio estimation problem, we propose a corresponding solution to boost performance for practical OOD detection instances.

In the following section, we first briefly introduce OOD detection.

2 OOD Detection

Given an in-distribution dataset $\mathcal{D}_{\text{in}} = \{x_1, \dots, x_N\}$, we would like to learn an OOD detector which can be formalised as an indicator function that maps a data x to $\{0, 1\}$:

$$D_\epsilon(x) = \begin{cases} 0 & s(x) < \epsilon; \\ 1 & s(x) \geq \epsilon, \end{cases}$$

where ϵ is a hyper-parameter which represents the confidence threshold and $s(x)$ is a score function representing whether or not a data x is likely to be an in-distribution sample. In practice, the threshold ϵ can be determined *e.g.* using the validation dataset. For evaluation, the Area Under the Receiver Operating Characteristics (AUROC) is calculated using the ID and OOD test datasets [13], automatically incorporating the consideration of different choices of ϵ value. Higher AUROC indicates that the detector has a better ability to discriminate between ID and OOD data.

2.1 Density-based OOD Detection

For the unsupervised OOD detection problem, a natural strategy is to learn a model $p_\theta(x)$ to fit the in-distribution dataset \mathcal{D}_{in} . The parameters θ can be learned by Maximum Likelihood Estimation

$$\theta^* = \arg \max_{\theta} \frac{1}{N} \sum_{n=1}^N p_\theta(x_n). \quad (1)$$

For a given test data x' , the density evaluation under the learned model $p_{\theta^*}(x')$ can be used as the score function for the OOD detection $s(x') \equiv p_{\theta^*}(x')$. In this case, lower density indicates that test data is more likely to be OOD [2]. Popular choices for the model p_θ are deep generative models such as Flow models [15, 17], latent variable models [16] or auto-regressive models [37]. However, recent work [30] shows the surprising result that deep generative models may assign *higher* density values to OOD data, that contain differing semantics, *c.f.* the ID data that was used for maximum likelihood

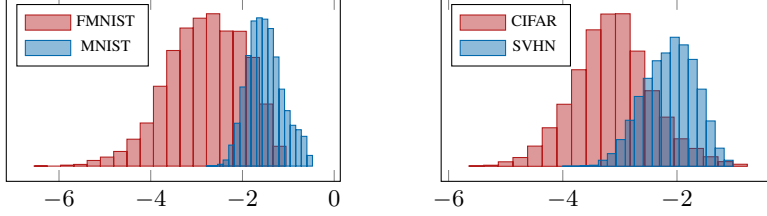


Figure 1: The left plot shows a PixelCNN model that is trained on FashionMNIST and tested on FashionMNIST (ID) and MNIST (OOD); the right plot show a PixelCNN model that is trained on CIFAR10 and tested on CIFAR10 (ID) and SVHN (OOD). The x -axis indicates the log-likelihood normalised by the data dimension and y -axis represents the data counts. We can observe that OOD datasets consistently obtain higher test likelihood than ID datasets. Plots are derived from [50].

training. Figure 1 shows an example of this effect where PixelCNN models trained on Fashion MNIST, CIFAR10 induce higher test likelihoods when evaluated on MNIST, SVHN respectively. Recently, many density ratio based methods [34, 17, 11, 50] are proposed, and achieve empirical success, where the score function is usually defined as the density ratio between two generative models p, q with different model structures. In the next section, we propose an energy-based model framework which enables a unified view of density ratio methods.

3 Unifying Density Ratio Methods with Energy-based Models

Recent work [50] proposes to model the in-distribution data using a product of local and non-local models and show that the non-local model can be considered a model of the data semantics. Here, we generalise this idea and define a general energy-based model for the in-distribution data, which in turn allows us to unify other density ratio-based OOD detection methods, such that they may be viewed as implicitly building semantic models on the in-distribution dataset.

We propose to model the in-distribution p_{in} with an energy-based model that can be defined as

$$p_{\text{in}}(x) = \frac{p_{\text{base}}(x)s(x)}{Z_{\text{in}}}, \quad \text{with} \quad Z_{\text{in}} = \int p_{\text{base}}(x)s(x)dx, \quad (2)$$

where p_{base} is the base distribution and $s(x)$ is a positive function that gives high score for the image x whose semantics belongs to the in-distribution p_{in} , such that the score function may be thought of in this case as a ‘semantic score’. A semantic distribution $p_s(x)$ can then be further defined as the normalised score function

$$p_s(x) = \frac{s(x)}{Z_s}, \quad \text{with} \quad Z_s = \int s(x)dx. \quad (3)$$

The density of the semantic distribution $p_s(x)$ can then be used to conduct semantic-level OOD detection. In practice, the estimation of the normalisation constant is not necessary for OOD detection tasks, since the score function is proportional to the likelihood ratio such that

$$s(x) \propto \frac{p_{\text{in}}(x)}{p_{\text{base}}(x)}, \quad (4)$$

so utilising the density ratio; $p_{\text{in}}(x)/p_{\text{base}}(x)$ is equivalent to using the semantic distribution $p_s(x)$ density value, in the context of OOD detection.

This model formulation is partially inspired by recent work [1, 4], where an energy-based model is defined using a trained Generative Adversarial Network (GAN) [8]. Specifically, given a trained generator $p_{\theta}(x) = \int p_{\theta}(x|z)p(z)dz$ and a real valued discriminator function $d(x)$ (where higher $d(x)$ values indicate that the generated sample x is closer to real data), an energy-based model can be defined

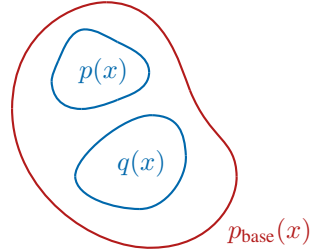


Figure 2: A visualisation of the energy based model. The real lines indicate the *high-density regions* of the distributions.

as $p_{\text{in}}(x) = \exp(d(x))p_{\theta}(x)/Z$, where the use of $\exp(\cdot)$ ensures positive density. In this case, the generator is also referred to as the ‘base distribution’ [1], which estimates the support of the data distribution and the weight function $\exp(d(x))$ (corresponding to our semantic score function $s(x)$) helps to ‘refine’ the density on the support. In contrast to a GAN-based energy model, where the support of the base distribution p_{base} is learned to be the support of the target data distribution p_d , the base distribution $p_{\text{base}}(x)$ in our model can alternatively cover a class of image distributions. For example, denote two image distributions as $p(x)$ and $q(x)$, our corresponding models are defined as

$$p(x) = \frac{p_{\text{base}}(x)s_p(x)}{Z_p}, \quad q(x) = \frac{p_{\text{base}}(x)s_q(x)}{Z_q}, \quad (5)$$

where each model is assumed to lie on the support of $p_{\text{base}}(x)$, yet the semantic score functions $s_p(\cdot)$ and $s_q(\cdot)$ are specific to the respective distributions, see Figure 2 for a visualization.

Several density-ratio based OOD methods can be unified under Equation 2 and the corresponding score can be explained as the (unnormalised) density of a semantic distribution that is defined by Equation 3. In the following methods that we discuss, p_{in} constitutes a generative model that is learned to fit the in-distribution data. Additionally various $p_{\text{base}}(x)$ have been proposed in the literature, which we also summarise below.

One definition of the base distribution $p_{\text{base}}(x)$ involves assigning *positive density for images with valid local features*. In [50], a *local model*, designed to only be capable of capturing local pixel dependency, is learned to realise $p_{\text{base}}(x)$. Similarly, [39, 40] propose to use classic lossless compressors, *e.g.* PNG or FLIF, to play the role of the local model. Since the PNG or FLIF format only use the neighbouring pixels to predict the target pixel [3], the resulting coding length for a given data x is approximately equal to the negative log-likelihood of a local model². In [11], the base model is defined as a hierarchical VAE which ignores the latent variable that incorporates the high-level features, so that the positive mass is assigned to images with valid low-level (local) features.

The base distribution $p_{\text{base}}(x)$ can also be defined to simply *assign mass to all valid images in a certain domain*. For example, if the in-distribution data were to consist of images containing horses, the domain can be defined as the distribution of animals. In practice, $p_{\text{base}}(x)$ is learned to fit a large image dataset which can represent the domain. The work of [39] used Flow+ [15] and PixelCNN [44] models, fitted to very large datasets, *e.g.* 80 Million Tiny Images dataset [7]. We refer to such distributions as *universal models*.

In comparison with the approaches surveyed so far, we note that the likelihood ratio method proposed by [34] does not fall under this framework. The authors alternatively assume that each data sample x can be factorised into two distinct components $x = \{x_b, x_s\}$, where x_b is a background component and x_s a semantic component. Two independent models $p(x_b), p(x_s)$ are then trained to model the two respective components. In contrast, our framework assumes that both functions $p_{\text{base}}(x), s(x)$ are supported on the x space.

We highlight that all discussed density estimation methods require the training of either one or two generative models. We argue that if the goal is to estimate the density ratio, training of complex generative models is not necessary. We propose to estimate the density ratio using the well-known class ratio estimation [42, 33, 10], which only requires learning of a binary classifier and thus significantly simplifies the OOD detection workflow during both training and testing procedures. In the following sections, we firstly give a brief introduction to class ratio estimation and then discuss practical considerations and applicability to the OOD detection task.

4 Model-Free Class Ratio Estimation

We denote distributions $p_{\text{in}}(x)$ and $p_{\text{base}}(x)$ as two conditional distributions $p(x|y=1)$ and $p(x|y=0)$ respectively, such that the density ratio becomes

$$\frac{p_{\text{in}}(x)}{p_{\text{base}}(x)} = \frac{p(x|y=1)}{p(x|y=0)}. \quad (6)$$

We define a mixture distribution $p(x)$ as $p(x) \equiv p(x|y=1)p(y=1) + p(x|y=0)p(y=0)$, where the Bernoulli prior distribution $p(y)$ represents the mixture proportions. We can further assume a

²See [27] for an introduction to the relationship between probabilistic modelling and lossless compression.

uniform prior $p(y = 1) = p(y = 0) = 0.5$ and rewrite Equation 6 using Bayes rule

$$\frac{p_{\text{in}}(x)}{p_{\text{base}}(x)} = \frac{p(x|y=1)}{p(x|y=0)} = \frac{p(y=1|x)p(x)}{p(y=0|x)p(x)} = \frac{p(y=1|x)}{p(y=0|x)}. \quad (7)$$

We are then ready to estimate the ratio using a binary classifier. We initially sample labelled data from $p(x, y) = p(x|y)p(y)$ by firstly sampling label $y' \sim p(y)$ and the corresponding data samples $x' \sim p(x|y = y')$. This is equivalent to sampling $x' \sim p_{\text{in}}$ when $y' = 1$ and $x' \sim p_{\text{base}}$ when $y' = 0$. The specified uniform prior $p(y)$ represents the probabilities to sample from p_{in} or p_{base} , which are equal. The generated data pairs are then used to train a probabilistic classifier $p_{\theta}(y|x)$ with the cross entropy loss, which has been shown to minimize the Bregman divergence between the ratio estimation $p_{\theta}(y=1|x)/p_{\theta}(y=0|x)$ and the true density ratio [29].

After training the classifier, the density ratio estimator $\frac{p_{\theta}(y=1|x)}{1-p_{\theta}(y=1|x)}$ can be used to perform OOD detection, thus avoiding the training of high-dimensional generative models. It may be observed that the class ratio estimation scheme requires samples from both distributions; p_{in} and p_{base} . The data samples of the in-distribution p_{in} are already provided. We next discuss how to obtain samples from p_{base} , according to the differing base distribution assumptions that were discussed in Section 3.

4.1 Construction of the base distribution

As previously discussed, training a binary classifier to estimate the ratio requires the samples from both p_{in} and p_{base} . Samples from p_{in} are just the in-distribution training dataset \mathcal{D}_{in} , which is given in the OOD detection task. We further discuss how to obtain the samples from p_{base} .

Recall, we propose that existing OOD ratio methods can be viewed as building energy-based model with different p_{base} distributions (Section 3). Specifically, these methods fall into two categories namely; (1) local model and (2) universal model base distributions. Therefore, we propose two corresponding methods to construct the samples from p_{base} , to form a dataset $\mathcal{D}_{\text{base}}$.

- **Local Model as Base Distribution** In principle, one can train a local generative model [50] on an image dataset and use that to generate local image samples, but this requires training a generative model. Alternatively, we propose to crop and resize the images from the given in-distribution dataset \mathcal{D}_{in} . Intuitively, cropping and resizing will preserve the local features, so the resulting images can be treated as the samples from a local model. We denote the resulting dataset as $\mathcal{D}_{\text{base}}^{\text{local}}$.
- **Universal Model as Base Distribution** The construction of samples from the universal model is more straightforward. We can simply use a large image dataset, *e.g.* 80 million tiny ImageNet [14] as our base distribution. We denote this large image data by $\mathcal{D}_{\text{base}}^{\text{uni}}$.

Under our model assumption described in Section 3, the support of p_{base} should contain the support of p_{in} , we thus intentionally include the samples from \mathcal{D}_{in} into the base distribution dataset by defining $\mathcal{D}_{\text{base}} = \mathcal{D}_{\text{base}}^{\text{local}} \cup \mathcal{D}_{\text{in}}$ or $\mathcal{D}_{\text{base}} = \mathcal{D}_{\text{base}}^{\text{uni}} \cup \mathcal{D}_{\text{in}}$. Further experimental details can be found in Section 5.

4.2 Spread Density Ratio Score

The semantic score that is used for OOD detection is defined by the density ratio $s(x) \propto p_{\text{in}}(x)/p_{\text{base}}(x)$. For a test data $x_{\text{test}} \notin \text{supp}(p_{\text{base}})$ ³, then $p_{\text{base}}(x_{\text{test}}) = 0$ and the ratio is not defined. Ideally, we want $p_{\text{base}}(x_{\text{test}})$ to have support that covers all possible x_{test} . One solution is to add convolutional Gaussian noise $\tilde{p}_{\text{base}} = p_{\text{base}} * p_n$, where p_n is an isotropic Gaussian distribution with mean 0 and variance $\sigma^2 I_D$, with data space dimension D . However, when using class-ratio estimation, there is a danger that the classifier can easily distinguish between samples from two distributions by simply considering the noise level, resulting in a poor estimation of the density ratio. This phenomenon is referred to as the ‘‘density-chasm’’ problem [35], in the class ratio estimation literature. To alleviate this problem, we propose to add the same convolutional noise to the distribution p_{in} : $\tilde{p}_{\text{in}} = p_{\text{in}} * p_n$. We can then define the *spread density ratio score* \tilde{s} :

$$\tilde{s}(x) = \frac{\tilde{p}_{\text{in}}(x)}{\tilde{p}_{\text{base}}(x)} = \frac{(p_{\text{in}} * p_n)(x)}{(p_{\text{base}} * p_n)(x)}. \quad (8)$$

³We use $\text{supp}(p)$ to denote the support of distribution p .

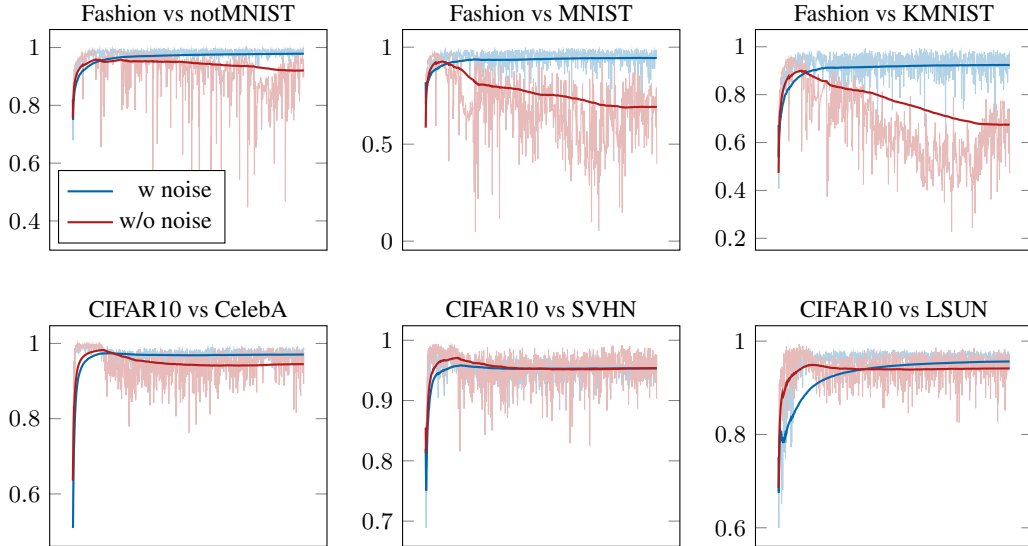


Figure 3: AUROC per epoch. The x -axis represents 1000 training epochs and y -axis represents the AUROC. The model is trained on $\mathcal{D}_{\text{in}} = \text{FashionMNIST} / \text{CIFAR10}$ and $\mathcal{D}_{\text{base}} = 80$ Million Tiny Images, then tested on the corresponding OOD datasets. We show that adding convolutional noise results in significantly more stable AUROC results.

Table 1: Comparison between local model and universal model as base distribution. From the table we can see that the universal model has better performance (AUROCs in %) in most of the ID-OOD pairs. Results are averaged over five runs.

ID dataset	OOD	Local	Universal	ID dataset	OOD	Local	Universal
FMNIST	MNIST	73.1	97.3	CIFAR10	SVHN	98.0	98.2
	NotMNIST	89.2	99.3		CIFAR100	54.7	85.9
	KMNIST	69.0	95.8		LSUN	37.0	97.3
	Omniglot	100.0	100.0		CelebA	58.3	96.5
MNIST	FMNIST	99.5	100.0	CIFAR100	SVHN	98.2	87.9
	NotMNIST	99.0	99.3		CIFAR10	47.7	64.4
	KMNIST	90.1	95.8		LSUN	95.0	83.8
	Omniglot	100.0	100.0		CelebA	38.5	90.5

When σ^2 is small, we assume that adding small pixel-wise noise to an image will not change the underlying semantics. Therefore $\tilde{s}(x)$ can still provide a valid representation of the semantic score. The name *spread density ratio* is inspired by recent work on spread divergences [49], where convolutional noise is added to two distributions with different supports in order to define a valid KL divergence. Adding noise to the samples from two distributions has also been used to stabilize the training of GANs [41].

When estimating the spread ratio $\tilde{s}(x)$ using the class-ratio estimation, we can sample from \tilde{p}_{in} by first taking $x \sim p_{\text{in}}, \epsilon \sim p_n$ and let $\tilde{x} = x + \epsilon$ define a sample from \tilde{p}_{in} . The same scheme is used to construct the samples from \tilde{p}_{base} . Section 5.3 provides empirical evidence to support the idea that the spread density ratio can significantly improve OOD detection results.

5 Experiments

In this section, we provide details of the implementations, the choice of datasets and the experimental results. The goal of our experiments is to demonstrate that for OOD detection tasks involving density ratios, a sole use of a binary classifier can achieve competitive performance, in relation to methods based on recent deep generative models.

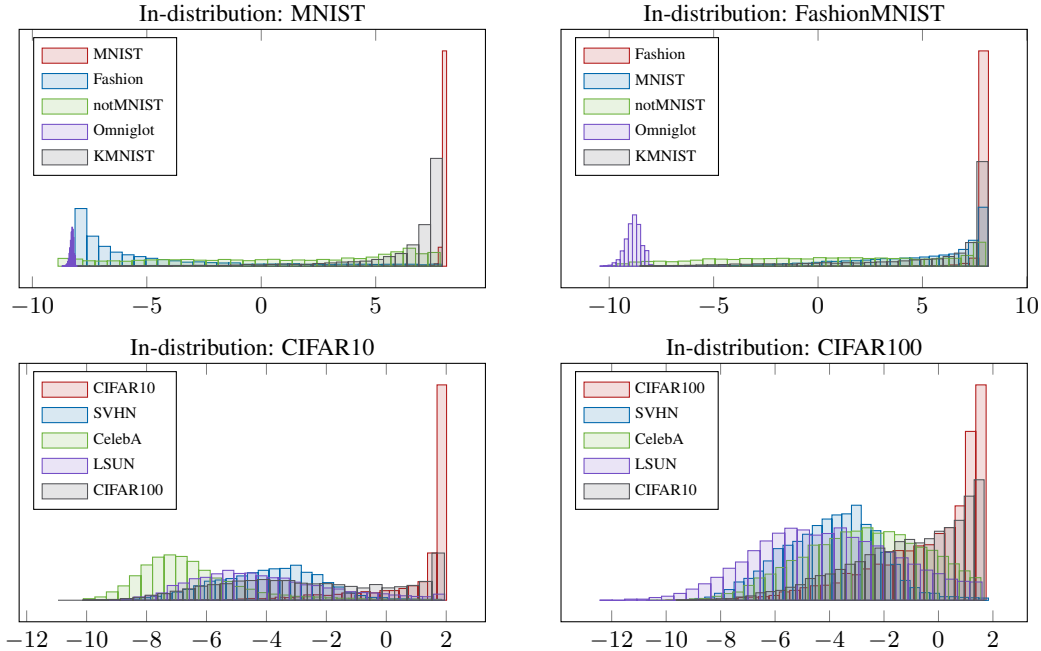


Figure 4: Histograms of the log density ratios on the test datasets when $\mathcal{D}_{\text{base}}$ is a universal model. We use red to indicate the in-distribution test set $\mathcal{D}_{\text{in}}^{\text{test}}$ and other colours represent different OOD test datasets $\mathcal{D}_{\text{out}}^{\text{test}}$. The x -axis is the log density ratio and the y -axis is the correspond count. We observe, for relatively better cases (MNIST / FashionMNIST / CIFAR10 as in-distribution), the density ratios of $\mathcal{D}_{\text{in}}^{\text{test}}$ are concentrated, while in the CIFAR100 case, the density ratios of $\mathcal{D}_{\text{in}}^{\text{test}}$ are spread out, with a large overlap with the density ratios of $\mathcal{D}_{\text{out}}^{\text{test}}$, leading to a relatively small AUROC.

Table 2: AUROC comparisons of approaches that use the additional 80 Million Tiny Images dataset, all results are averaged over five runs. Both Outlier Exposure (OE) [14] and Tiny-Glow/PCNN [39] require training complex generative models. We observe our method achieves competitive performance without requiring any generative model training.

ID	OOD	OE [14]	Tiny-Glow [39]	Tiny-PCNN [39]	Ours
CIFAR10	SVHN	75.8	93.9	94.4	98.2
	CIFAR100	68.5	66.8	63.5	85.9
	LSUN	90.9	89.2	92.9	97.3
CIFAR100	SVHN	-	87.4	90.0	87.9
	CIFAR10	-	52.8	54.5	64.4
	LSUN	-	81.0	87.6	83.8

5.1 Neural Network Structure and Training Details

As introduced in Section 4, our model is a binary classifier estimating $p(y = 1|x)$. We use ResNet-18 [12] for greyscale experiments and WideResNet-28-10 [48] for colour image experiments. The classifiers are trained for 1000 epochs using a learning rate of 0.01, batch size of 256, and a Stochastic Gradient Descent(SGD) optimizer [36] with momentum = 0.9. The implementation can be found in our anonymous public repo⁴. All experiments are conducted on a NVIDIA Tesla V100 GPU.

Following recent work [13], we select MNIST [22], FashionMNIST [45], CIFAR10 and CIFAR100 [18] to be in-distribution datasets \mathcal{D}_{in} , respectively. We use OMNIGLOT [20], KMNIST [6] and notMNIST as OOD test datasets $\mathcal{D}_{\text{out}}^{\text{test}}$ for greyscale experiments and we select SVHN [32], LSUN [47] and CelebA [26] as $\mathcal{D}_{\text{out}}^{\text{test}}$ for colour image experiments.

⁴<https://github.com/andiac/OODRatio>

5.2 Effectiveness of Spread Density Ratio

As discussed in Section 4.2, we add Gaussian noise to both p_{in} and p_{base} in the training stage and use the resulting spread density ratio to represent the semantic density. We apply Gaussian noise with standard deviation 0.1 for both greyscale and colour image experiments. For p_{base} , we use a universal model (described in Section 4.1). Universal model sample construction details can be found in Section 5.3. Fig. 3 compares the test AUROC after each training epoch. We see that adding spread noise can significantly improve the distinguishability and training stability, for both datasets.

5.3 Comparison Between Two Base Distributions

In this section, we compare two base distributions introduced in Section 4.1: namely the local model and universal model. For the local model, samples are constructed by random cropping and resizing. In greyscale experiments, we crop the 28×28 images from \mathcal{D}_{in}^{train} into $14 \times 14 / 16 \times 16 / \dots / 24 \times 24 / 26 \times 26$ images randomly, and then resize back to 28×28 using bilinear interpolation. Similarly, in colour image experiments, we crop the 32×32 images into $16 \times 16 / \dots / 30 \times 30$ images randomly, then resize back to the original size, analogously. The resulting images are denoted as $\mathcal{D}_{base}^{local}$.

For the universal model, we use a cleaned⁵ subset of the 80 Million Tiny Images dataset [43], resulting in 300K images [14], that serve as our samples from a universal model, which ensures the diversity of \mathcal{D}_{base}^{uni} [14]. For grey-scale experiments (*i.e.* when \mathcal{D}_{in} is FashionMNIST or MNIST), we convert the 80 Million Tiny Images dataset to greyscale as our \mathcal{D}_{base}^{uni} .

Table 1 shows the AUROC comparison for two p_{base} constructions. We find that our local model sample construction can achieve strong results in several cases; CIFAR *v.s.* SVHN, MNIST *v.s.* all and FashionMNIST *v.s.* NotMNIST / Omniglot. However, performance is more modest in several cases such as CIFAR10 *v.s.* CIFAR100 / LSUN / CelebA or CIFAR100 *v.s.* CIFAR10 / CelebA. In contrast, the samples from the universal model achieves strong performance in all experiments. We conjecture that our constructed local samples cannot comprehensively characterise the underlying local model (*i.e.* a model which can assign positive density to *all* images with valid features). We believe the question of how to construct better local samples to be a promising future research direction.

5.4 Comparisons with Other Methods

We compare our approach, that defines p_{base} using the universal model, with methods that also assume access to the Tiny-imagenet dataset, see Table 2. We observe that our method achieves relatively improved performance in four out of six ID-OOD pairs (see Fig. 4 for corresponding histogram plots). Tiny-PCNN [39] achieves better performance in two data pairs, however, in contrast to our approach, we note that it requires training of two deep generative models.

We also compare our method to other recently proposed unsupervised OOD detection approaches, which include density ratio methods. In Table 3, we report the number of generative models that each require to train. We observe that our method, with universal model, achieves competitive performance without training any generative models, providing computational efficiency.

Table 3: AUROC comparisons. We report the number of generative models used by alternative approaches in the third column. It may be observed that our model achieves relatively strong performance, (uniquely) without use of any generative models. Results for the Typicality test [40] correspond to batches of two samples of the same type. All results are averaged over five runs.

ID: OOD :	FMNIST MNIST	CIFAR10 SVHN	Gen.
WAIC [5]	76.6	100.0	5
Like. Regret [46]	98.8	87.5	1
HVAE [11]	98.4	89.1	1
MSMA KD [28]	69.3	99.1	1
OE [14]	-	75.8	1
Density Ratio-based Methods			
Like. Ratio[34]	99.7	91.2	2
Glow/PNG [39]	-	75.4	1
PCNN/PNG [39]	-	82.3	1
Glow/FLIF [40]	99.8	95.0	1
PCNN/FLIF [40]	96.7	92.9	1
Global/Local[50]	100.0	96.9	2
Glow/Tiny [39]	-	93.9	2
PCNN/Tiny [39]	-	94.4	2
Ours-Local	73.1	97.2	0
Ours-Universal	97.3	98.2	0

⁵Cleaning follows the strategy suggested by [14] and removes images from the 80 Million Tiny Images dataset that belong to classes pertaining to CIFAR, LSUN and Places datasets.

6 Conclusion

In this work, we propose an energy-based model framework that affords a unified modelling view of the recently proposed density-ratio based OOD methods. We further propose to use the class ratio estimation to estimate the density ratio, which does not require the training of complex generative models and yet can still achieve competitive OOD detection results, in comparison with state-of-the-art approaches. Our work gives rise to new potential directions *e.g.* more rigorous investigation of how to construct p_{base} , which we leave to future work.

References

- [1] M. Arbel, L. Zhou, and A. Gretton. Generalized energy based models. *arXiv preprint arXiv:2003.05033*, 2020.
- [2] C. M. Bishop. Novelty detection and neural network validation. *IEE Proceedings-Vision, Image and Signal processing*, 141(4):217–222, 1994.
- [3] T. Boutell. Png (portable network graphics) specification version 1.0. Technical report, 1997.
- [4] T. Che, R. Zhang, J. Sohl-Dickstein, H. Larochelle, L. Paull, Y. Cao, and Y. Bengio. Your gan is secretly an energy-based model and you should use discriminator driven latent sampling. *Advances in Neural Information Processing Systems*, 33:12275–12287, 2020.
- [5] H. Choi, E. Jang, and A. A. Alemi. Waic, but why? generative ensembles for robust anomaly detection. *arXiv preprint arXiv:1810.01392*, 2018.
- [6] T. Clanuwat, M. Bober-Irizar, A. Kitamoto, A. Lamb, K. Yamamoto, and D. Ha. Deep learning for classical japanese literature, 2018.
- [7] J. Deng, W. Dong, R. Socher, L.-J. Li, K. Li, and L. Fei-Fei. Imagenet: A large-scale hierarchical image database. In *2009 IEEE conference on computer vision and pattern recognition*, pages 248–255. Ieee, 2009.
- [8] I. Goodfellow, J. Pouget-Abadie, M. Mirza, B. Xu, D. Warde-Farley, S. Ozair, A. Courville, and Y. Bengio. Generative adversarial nets. *Advances in neural information processing systems*, 27, 2014.
- [9] C. Guo, G. Pleiss, Y. Sun, and K. Q. Weinberger. On calibration of modern neural networks. *arXiv preprint arXiv:1706.04599*, 2017.
- [10] M. Gutmann and A. Hyvärinen. Noise-contrastive estimation: A new estimation principle for unnormalized statistical models. In *Proceedings of the Thirteenth International Conference on Artificial Intelligence and Statistics*, pages 297–304, 2010.
- [11] J. D. D. Havtorn, J. Frellsen, S. Hauberg, and L. Maaløe. Hierarchical vaes know what they don’t know. In *International Conference on Machine Learning*, pages 4117–4128. PMLR, 2021.
- [12] K. He, X. Zhang, S. Ren, and J. Sun. Deep residual learning for image recognition. In *Proceedings of the IEEE conference on computer vision and pattern recognition*, pages 770–778, 2016.
- [13] D. Hendrycks and K. Gimpel. A baseline for detecting misclassified and out-of-distribution examples in neural networks. *arXiv preprint arXiv:1610.02136*, 2016.
- [14] D. Hendrycks, M. Mazeika, and T. Dietterich. Deep anomaly detection with outlier exposure. *arXiv preprint arXiv:1812.04606*, 2018.
- [15] D. P. Kingma and P. Dhariwal. Glow: Generative flow with invertible 1x1 convolutions. *arXiv preprint arXiv:1807.03039*, 2018.
- [16] D. P. Kingma and M. Welling. Auto-encoding variational bayes. *arXiv preprint arXiv:1312.6114*, 2013.

- [17] P. Kirichenko, P. Izmailov, and A. G. Wilson. Why normalizing flows fail to detect out-of-distribution data. *arXiv preprint arXiv:2006.08545*, 2020.
- [18] A. Krizhevsky, G. Hinton, et al. Learning multiple layers of features from tiny images. 2009.
- [19] M. Kull, M. P. Nieto, M. Kängsepp, T. Silva Filho, H. Song, and P. Flach. Beyond temperature scaling: Obtaining well-calibrated multi-class probabilities with dirichlet calibration. In *Advances in neural information processing systems*, pages 12316–12326, 2019.
- [20] B. M. Lake, R. Salakhutdinov, and J. B. Tenenbaum. Human-level concept learning through probabilistic program induction. *Science*, 350(6266):1332–1338, 2015.
- [21] B. Lakshminarayanan, A. Pritzel, and C. Blundell. Simple and scalable predictive uncertainty estimation using deep ensembles. In *Advances in neural information processing systems*, pages 6402–6413, 2017.
- [22] Y. LeCun, L. Bottou, Y. Bengio, and P. Haffner. Gradient-based learning applied to document recognition. *Proceedings of the IEEE*, 86(11):2278–2324, 1998.
- [23] K. Lee, K. Lee, H. Lee, and J. Shin. A simple unified framework for detecting out-of-distribution samples and adversarial attacks. In *Advances in Neural Information Processing Systems*, pages 7167–7177, 2018.
- [24] S. Liang, Y. Li, and R. Srikant. Enhancing the reliability of out-of-distribution image detection in neural networks. *arXiv preprint arXiv:1706.02690*, 2017.
- [25] W. Liu, X. Wang, J. D. Owens, and Y. Li. Energy-based out-of-distribution detection. *arXiv preprint arXiv:2010.03759*, 2020.
- [26] Z. Liu, P. Luo, X. Wang, and X. Tang. Deep learning face attributes in the wild. In *Proceedings of International Conference on Computer Vision (ICCV)*, December 2015.
- [27] D. J. MacKay, D. J. Mac Kay, et al. *Information theory, inference and learning algorithms*. Cambridge university press, 2003.
- [28] A. Mahmood, J. Oliva, and M. Styner. Multiscale score matching for out-of-distribution detection. *arXiv preprint arXiv:2010.13132*, 2020.
- [29] A. Menon and C. S. Ong. Linking losses for density ratio and class-probability estimation. In *International Conference on Machine Learning*, pages 304–313. PMLR, 2016.
- [30] E. Nalisnick, A. Matsukawa, Y. W. Teh, D. Gorur, and B. Lakshminarayanan. Do deep generative models know what they don’t know? *International Conference on Learning Representations*, 2019.
- [31] E. Nalisnick, A. Matsukawa, Y. W. Teh, and B. Lakshminarayanan. Detecting out-of-distribution inputs to deep generative models using a test for typicality. *arXiv preprint arXiv:1906.02994*, 5, 2019.
- [32] Y. Netzer, T. Wang, A. Coates, A. Bissacco, B. Wu, and A. Y. Ng. Reading digits in natural images with unsupervised feature learning. 2011.
- [33] J. Qin. Inferences for case-control and semiparametric two-sample density ratio models. *Biometrika*, 85(3):619–630, 1998.
- [34] J. Ren, P. J. Liu, E. Fertig, J. Snoek, R. Poplin, M. Depristo, J. Dillon, and B. Lakshminarayanan. Likelihood ratios for out-of-distribution detection. In *Advances in Neural Information Processing Systems*, pages 14707–14718, 2019.
- [35] B. Rhodes, K. Xu, and M. U. Gutmann. Telescoping density-ratio estimation. *arXiv preprint arXiv:2006.12204*, 2020.
- [36] H. Robbins and S. Monro. A stochastic approximation method. *The annals of mathematical statistics*, pages 400–407, 1951.

- [37] T. Salimans, A. Karpathy, X. Chen, and D. P. Kingma. Pixelcnn++: Improving the pixelcnn with discretized logistic mixture likelihood and other modifications. *arXiv preprint arXiv:1701.05517*, 2017.
- [38] C. S. Sastry and S. Oore. Detecting out-of-distribution examples with in-distribution examples and gram matrices. *arXiv preprint arXiv:1912.12510*, 2019.
- [39] R. Schirrmeister, Y. Zhou, T. Ball, and D. Zhang. Understanding anomaly detection with deep invertible networks through hierarchies of distributions and features. *Advances in Neural Information Processing Systems*, 33:21038–21049, 2020.
- [40] J. Serrà, D. Álvarez, V. Gómez, O. Slizovskaia, J. F. Núñez, and J. Luque. Input complexity and out-of-distribution detection with likelihood-based generative models. *arXiv preprint arXiv:1909.11480*, 2019.
- [41] C. K. Sønderby, J. Caballero, L. Theis, W. Shi, and F. Huszár. Amortised map inference for image super-resolution. *arXiv preprint arXiv:1610.04490*, 2016.
- [42] M. Sugiyama, T. Suzuki, and T. Kanamori. *Density ratio estimation in machine learning*. Cambridge University Press, 2012.
- [43] A. Torralba, R. Fergus, and W. T. Freeman. 80 million tiny images: A large data set for nonparametric object and scene recognition. *IEEE transactions on pattern analysis and machine intelligence*, 30(11):1958–1970, 2008.
- [44] A. Van Oord, N. Kalchbrenner, and K. Kavukcuoglu. Pixel recurrent neural networks. In *International conference on machine learning*, pages 1747–1756. PMLR, 2016.
- [45] H. Xiao, K. Rasul, and R. Vollgraf. Fashion-mnist: a novel image dataset for benchmarking machine learning algorithms. *arXiv preprint arXiv:1708.07747*, 2017.
- [46] Z. Xiao, Q. Yan, and Y. Amit. Likelihood regret: An out-of-distribution detection score for variational auto-encoder. *Advances in neural information processing systems*, 33:20685–20696, 2020.
- [47] F. Yu, Y. Zhang, S. Song, A. Seff, and J. Xiao. Lsun: Construction of a large-scale image dataset using deep learning with humans in the loop. *arXiv preprint arXiv:1506.03365*, 2015.
- [48] S. Zagoruyko and N. Komodakis. Wide residual networks. *arXiv preprint arXiv:1605.07146*, 2016.
- [49] M. Zhang, P. Hayes, T. Bird, R. Habib, and D. Barber. Spread divergence. In *International Conference on Machine Learning*, pages 11106–11116. PMLR, 2020.
- [50] M. Zhang, A. Zhang, and S. McDonagh. On the out-of-distribution generalization of probabilistic image modelling. *Advances in Neural Information Processing Systems*, 34, 2021.